



Robust in-fiber spatial interferometer using multicore fiber for vibration detection

ZHIYONG ZHAO,^{1,*} ZHENGYONG LIU,² MING TANG,³ SONGNIAN FU,³ LIANG WANG,⁴ NAN GUO,¹ CHAO JIN,¹ HWA-YAW TAM,² AND CHAO LU¹

¹Photonics Research Centre, Department of Electronic and Information Engineering, The Hong Kong Polytechnic University, Hong Kong, China

²Department of Electrical Engineering, The Hong Kong Polytechnic University, Hong Kong, China

³National Engineering Laboratory of Next Generation Internet Access Networks, School of Optical and Electronic Information, Huazhong University of Science and Technology, Wuhan 430074, China

⁴Department of Electrical Engineering, The Chinese University of Hong Kong, Hong Kong, China

*zhiyong.zhao@polyu.edu.hk

Abstract: We report the demonstration of a novel in-fiber spatially integrated Michelson interferometer based on weakly coupled multicore fiber (MCF) for vibration sensing. The compact interferometer is constructed by using two separate cores of the MCF, where the fiber end is cleaved in order to generate strong Fresnel reflection, and independent light coupling between the cores of MCF and the single mode fibers (SMFs) is enabled by the fan-in coupler. Vibration gives rise to differential strain variation between cores which results in the modification of phase difference of the interferometer. A narrow linewidth laser is employed, in order to interrogate the phase change induced reflection power variation. Vibration event can be identified and the vibration frequency can be retrieved by processing the measured reflection power with fast Fourier transform (FFT). Broad vibration frequency response range up to 12 kHz (limited by the cut-off frequency of the voltage driver of the vibration source) has been achieved. Performance of the sensor has been shown to be independent of the selection of different core pairs, where the MCF is wound to a piezoelectric transducer (PZT). The proposed in-fiber integrated spatial interferometer does not require any special processing of the fiber (e.g., tapering, splicing, and so forth). The unique sensor structure provides some extraordinary merits, including ultra-compact size, high mechanical strength, high sensitivity and temperature insensitivity.

© 2018 Optical Society of America under the terms of the [OSA Open Access Publishing Agreement](#)

1. Introduction

Vibration detection is a widely used diagnosis and/or assessment method in many application fields, such as structure health monitoring, seismic monitoring and security monitoring. It helps to predict the potential threat of structural failure through real-time monitoring the characteristic frequency of vibration of the structure. By monitoring the underground vibration, the in-field seismic wave measurement provides useful information for oil and gas exploration, as well as for early prediction of earthquakes. In addition, it has also been used for security monitoring by extracting the vibration information on the ground or walls. The traditional piezoelectric vibration sensors suffer from a number of drawbacks, including sensitive to electromagnetic fields, not adaptable for harsh environments (e.g. high temperature, corrosive environment, etc.), difficult to carry out multiplexing. Optical fiber vibration sensor (OFVS) has shown great potential in these application fields, and it has undergone a rapid development in the past two decades, owing to its unique advantages, including intrinsic electrical passivity, immunity to electromagnetic interference, chemical resistance, light weight, small size and remote access ability. So far, various configurations of OFVS have been developed. One of the most widely used schemes is the tapered fiber based vibration sensors [1–4], where either the tapered fiber is used as the sensing arm of the Mach–

Zehnder interferometers or the microbending loss of the tapered fiber is utilized to detect vibration. However, the tapered fibers are fragile, which results in poor mechanical strength of the sensor head. Fiber Bragg gratings have also been extensively used for vibration sensing [5–8]. It normally requires a wavelength scanning light source to demodulate the Bragg reflection wavelength, so the detectable frequency range is usually quite limited. In addition, modal interferometers which are fabricated by splicing different kinds of fibers have also been demonstrated [9–12]. However, the concern is that this kind of sensors has bad mechanical strength due to splicing.

In this work, we propose and experimentally demonstrate a novel in-fiber spatially integrated Michelson interferometer (MI) by employing weakly coupled multicore fiber and a fan-in coupler, where the fiber end is cleaved to generate sufficient Fresnel reflection, and two separate spatial cores of the MCF is employed to construct the single fiber embedded MI configuration. The proposed compact MI has been used for vibration sensing, and broad vibration frequency response range up to 12 kHz (limited by the cut-off frequency of the voltage driver of the PZT) has been achieved. The vibration responses of MIs constructed using different core pairs have been experimentally compared. The results show that the selection of fiber core pairs has no effect on the determination of vibration frequency. Thanks to the unique in-fiber integrated spatial interferometer configuration with independent light coupling enabled by the fan-in coupler, the proposed sensor does not require any special processing of the fiber (e.g. tapering, splicing, etc.). This gives it the advantages of compact size, high mechanical strength, high sensitivity and temperature-insensitivity.

2. Working principle of in-fiber spatially integrated MI vibration sensor using MCF

Figure 1 shows the cross sectional view of the MCF (YOFC, China) used in our experiments. It contains seven cores with the outer six cores arranged hexagonally. The cladding diameter of the MCF is 150 μm and the core-core pitch is 42 μm . The cores are surrounded by deep trench in order to suppress crosstalk, where $-45\text{dB}/100\text{km}$ crosstalk between adjacent cores has been achieved [13].



Fig. 1. Cross sectional view of the multi-core fiber used in the experiment.

In the proposed MCF based spatially integrated Michelson interferometer, sufficient Fresnel reflection is enabled by cleaving the fiber end, and two independent cores of the MCF constitute the arms of the MI. The output electric fields of light from the two cores are given by $E_1(t)\exp[j(\omega t + \varphi_1(t))]$ and $E_2(t)\exp[j(\omega t + \varphi_2(t))]$, then the output reflection power $I(t)$ of the MI is governed by [14]:

$$I(t) = |E_1(t)|^2 + |E_2(t)|^2 + 2|E_1(t)||E_2(t)|\cos(\Delta\varphi(t)) \quad (1)$$

where $E_1(t)$ and $E_2(t)$ are the amplitudes of electric fields of light in the two cores, ω is the optical angular frequency, $\varphi_1(t)$ and $\varphi_2(t)$ are the optical phases of light, and $\Delta\varphi(t)$ is the optical phase difference that is given by:

$$\Delta\varphi(t) = \varphi_1(t) - \varphi_2(t) = \frac{4\pi n \Delta l}{\lambda} \quad (2)$$

where n is the effective refractive index of the fiber core, Δl is the length difference between the two arms, and λ is the wavelength of the input light.

Vibration induced displacement will lead to the change of curvature of the MCF. When the MCF is bent, the cores at off-center positions (i.e. the six outer cores) will be either stretched or compressed, as shown in Fig. 2. This will cause local tangential strain at the bending point, and the generated strain ε_i in a specific core i is angular position dependent, as given by [15]:

$$\varepsilon_i = -\frac{d}{R} \cos(\theta_b - \theta_i) \quad (3)$$

where d is the distance of core i to the fiber center, R is the bending radius, θ_b is the bending angle and θ_i is the angular position of core i [15]. Specifically, as shown in Fig. 2, the cores on the outer side of the neutral plane will be elongated [e.g. core A in Fig. 2], while the cores on the inner side of the neutral plane will be compressed [e.g. core B in Fig. 2]. So if the curvature of the MCF changes, the length difference Δl between the two cores of the MI will vary as well. Meanwhile the effective refractive index n of the fiber cores will also change due to the bending induced tangential strain. As a result, the optical phase difference $\Delta\varphi(t)$ between the two cores of the MI will be changed, and the interfered output of the MI will vary with vibration. Therefore, by monitoring the variation of output power of the MI over time, the vibration frequency can be obtained.

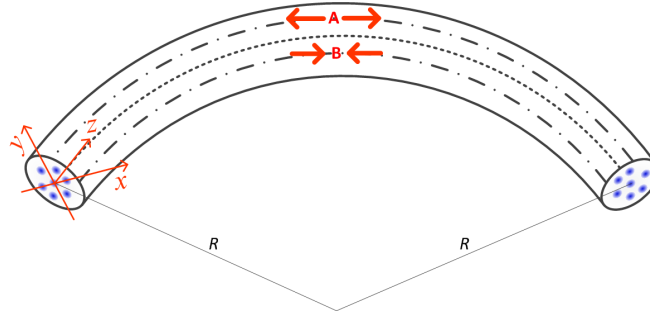


Fig. 2. Schematic diagram of the bent MCF with a bending radius of R . Core A and Core B represent the elongated outer side core and the compressed inner side core, respectively.

It must be pointed out that the other reported interferometric vibrations sensors that are fabricated by either splicing or tapering are essentially based on the principle of light interference between different optical modes (including super-modes) within a single optical path in the fiber [3,9–12]. However, different from previously reported interferometric vibrations sensors, the proposed MCF based in-fiber spatially integrated MI is fabricated by using two independent cores of a single fiber, where two completely separate optical paths are employed to construct the interferometer, and independent light coupling between the cores of MCF and the SMFs is enabled by the fan-in coupler. The vibration-sensitivity is essentially caused by the differential strains between the cores that result from the vibration induced structural deformation of the MCF. So the fundamental working principle of the proposed MI sensor is different from the other reported interferometric sensors, and the work presented in this paper reveals a novel approach to fabricate optical fiber interferometers based on spatially integrated configuration within a single fiber, which will find various applications in bending measurement, and many other parameters that are related to bending, such as

vibration, acceleration, flow velocity of liquid and gas, etc [16]. The proposed sensor offers the unique advantage of high mechanical strength in comparison with other sensors that are fabricated by splicing or tapering, which is very important in field deployments of the fiber sensors.

3. Experimental setup, results, and discussions

The experiment setup used for the weakly coupled MCF based spatially integrated Michelson interferometer vibration sensor is shown in Fig. 3. A narrow linewidth distributed feedback (DFB) laser with 10.9 dBm output power is used in the system, which is connected to a 2x2 coupler. Light from the two output ports of the coupler is then launched into two cores of the MCF through a fan-in coupler, which contains seven single mode fiber pigtailed and a MCF pigtail. The fan-in coupler ensures independent optical coupling from one SMF pigtail to a specific core of the MCF [17,18]. The output reflected light from the MCF is detected by a 125 MHz photodetector, and an oscilloscope is used to acquire the data. The length of MCF used in the experiment is about 3 m for the convenience of delivering light, but in fact much shorter fiber length should be sufficient to implement the MI vibration sensor. While on the other hand, longer fiber length can be used in order to construct a zone-type vibration sensor for the application of perimeter security. A section of the MCF is wound to a cylindrical PZT with about seven rings in order to apply vibration, and the PZT has a diameter of 4 cm. It should be pointed out that in order to protect the multicore fiber from being broken, one should avoid too small bending radius in the deployment of the fiber sensor. In order to obtain sufficient Fresnel reflection, the end face of MCF has been cleaved, and the reflectivity of each core has been measured, as presented in Table 1. Note that the average insertion loss for each core of the MCF fan-in coupler is about 1.5 dB. It turns out that despite the different reflectivities between the cores, which is caused by the uneven fiber end, the generated Fresnel reflections are all sufficient for sensing already. In addition, a film with high reflectivity can be coated to the cleaved fiber end in order to increase the Fresnel reflection.

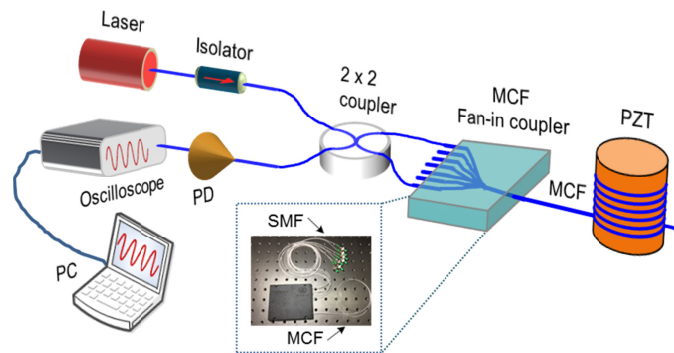


Fig. 3. Experimental setup for the MCF based Michelson interferometer vibration sensor. PD: photodetector; PC: personal computer. The inset shows the packaged MCF fan-in coupler.

Table 1. The measured reflectivity of each core of the MCF

Core No.	Core 1	Core 2	Core 3	Core 4	Core 5	Core 6	Core 7
Reflectivity	-22.4 dB	-27.4 dB	-25.3 dB	-24.2 dB	-21 dB	-25.2 dB	-30.8 dB

The PZT is driven by a high voltage driver, which is connected to an arbitrary waveform generator so as to apply periodic sinusoidal signal. In order to investigate the response performance of the proposed sensor configuration, the MI that consists of core 2 and core 5 [see Fig. 1] has been used for vibration test. Figure 4(a) shows the measured time-domain power signal of the MI in one second when a 7 kHz sinusoidal vibration signal is applied to the PZT. The zoom-in view of Fig. 4(a) is shown in Fig. 4(b) in red solid line, and the dashed

line in light blue is the sinusoidal fitting of the sampled waveform. The time-domain power signal is then processed by fast Fourier transform, and the retrieved frequency spectrum is presented in Fig. 4(c). The dominant peak in the figure appears at 7 kHz, which agrees well with the applied frequency value. In addition, 37 dB signal-to-noise ratio (SNR) has been achieved, which indicates that the proposed sensor possesses enough SNR budget to enable the measurement of higher vibration frequency.

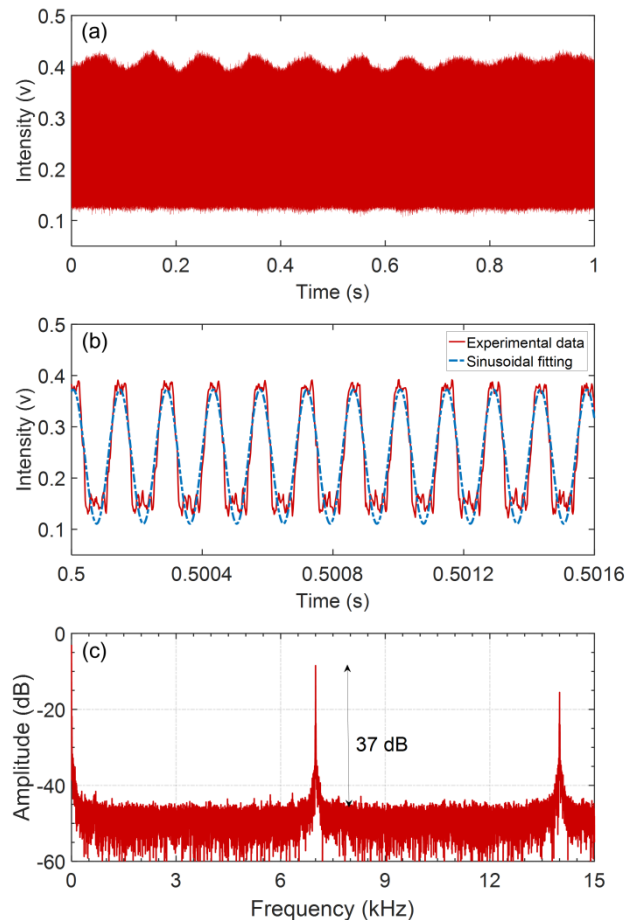


Fig. 4. (a) The measured time-domain power signal of the MI within 1 second when 7 kHz vibration is applied on the MCF; (b) zoom-in view of the optical power spectrum; (c) the retrieved frequency spectrum obtained by FFT.

In order to further evaluate the performance of the proposed MI sensor for vibration sensing, experiments have been carried out by applying different vibration frequency to the PZT from 1 kHz to 12 kHz at 1 kHz interval. The load voltage of PZT is fixed at the same value when different vibration frequency is applied. The output time-domain power signals of the MI at different vibration frequencies are sampled and processed by FFT, respectively. The retrieved FFT spectra are shown in Fig. 5. The result verifies the excellent measurement accuracy of the proposed MI sensor in terms of the determination of vibration frequency. It also indicates that high SNR can be obtained by the sensor, even when the vibration frequency is very high (e.g. 12 kHz in the figure). In addition, it should be pointed out that the electric cut-off frequency of the high voltage driver of the PZT is less than 13 kHz, which determines the maximum available vibration frequency in the lab. Due to sufficient SNR

offered by the MCF spatially integrated MI configuration, it is believed that the proposed sensor is able to measure vibrations at much higher frequencies.

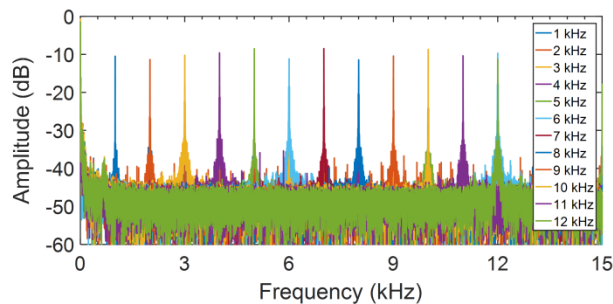


Fig. 5. FFT spectra of the power signal measured by the MI vibration sensor when vibration is applied to the sensing fiber with vibration frequency from 1 kHz to 12 kHz at 1 kHz interval.

In order to investigate the vibration response characteristics of the spatially integrated MI configurations using different core pairs, experiments have been conducted by selecting distinct combinations of two cores to construct the MIs, and then use them to measure vibration respectively. Due to the symmetrical distribution of cores of the MCF, we choose the core pairs with 60° angular offset (i.e. core 2 and core 7), 120° angular offset (i.e. core 2 and core 6), 180° angular offset (i.e. core 2 and core 5), as well as the combination of one outer core and the center core (i.e. core 2 and core 1) in the experiment to investigate the dependence of performance on core pairs. The MIs that consist of different core pairs have been used to measure a 2 kHz vibration, respectively. In the experiment, the output signals of the MIs are recorded and processed by FFT, respectively. The obtained FFT spectra are presented in Fig. 6. The SNRs of the FFT spectra are 23.1 dB, 23.49 dB, 22.75 dB and 20.4 dB for core2-core1, core2-core5, core2-core6 and core2-core7, respectively. It is founded that all MIs using different core pairs are able to retrieve the correct vibration frequency, thus it indicates that the determination of vibration frequency of the MI sensor is independent of the selection of different core pairs. It is worth noting that the vibration amplitude is small here, since the amount of diameter change caused by PZT is actually very small in the experiments. However, owing to the fact that the strong Fresnel reflection brings in sufficient optical power to the photodetector, which ensures high SNR for the measured time-domain waveforms of the interferometer. Additionally, since about seven rings of MCF have been wound to the PZT, the vibration induced accumulated phase change is actually large for all the cores, and this has resulted in high fringe contrast of the measured interference waveforms. That's why high SNRs have been obtained for all the measurements using different core pairs.

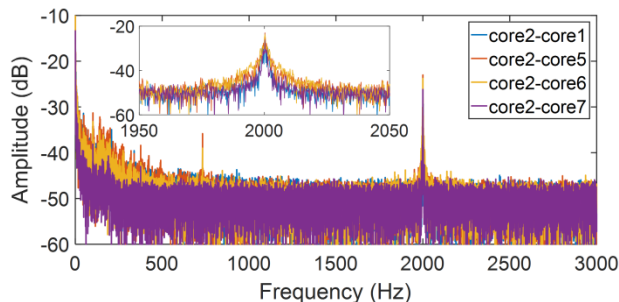


Fig. 6. FFT spectra obtained by the MI sensors using different core pairs when 2 kHz vibration is applied to the MCF. The inset shows the zoom-in view of frequency spectrum around 2 kHz.

Since the MI structure is very sensitive to optical phase change, the wavelength drift induced phase fluctuation of the laser source might be a factor that degrades the performance of the proposed vibration sensor. In order to investigate the impact of laser phase noise on the reliability of system, experiment has been carried out for comparison by monitoring the output signal of the sensor when there is no vibration applied to the sensing fiber. Figure 7(a) shows the measured output power of the MI without vibration applied, where two separate measurements have been presented. It is found that due to random wavelength drift of the laser, the output power of the MI shows slight change over time when there is no vibration applied to the MCF. The frequency spectra of the two measurements are then obtained by calculating the FFT, as shown in Fig. 7(b). The result indicates that the laser phase fluctuation induced frequency noise of the sensor has very weak power spectrum amplitude, and the noise floor is less than -40 dB in the frequency region that is higher than 200 Hz. Therefore, the laser wavelength drift induced phase noise will not cause severely detrimental impact on the measurement.

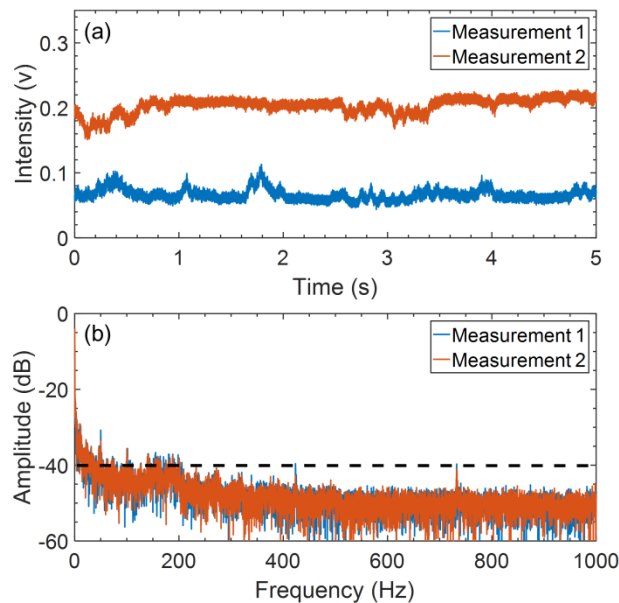


Fig. 7. (a) The measured time-domain power signals of the MI when there is no vibration applied to the sensing fiber; (b) the retrieved frequency spectra obtained by FFT.

It is worth mentioning that the in-fiber spatially integrated MI configuration also provides another advantage of temperature insensitivity. Because the MCF used here is a homogeneous MCF, whose fiber cores are made from the same preform. So they have the same thermal expansion coefficients and thermo-optic coefficients. Since the two arms of the proposed MI are embedded in the same fiber cladding. So they will undergo the same environmental temperature change, and this will lead to identical phase change of light in the two arms. As a result, the sensor response is immune to the temperature variation, and this will help to enhance the reliability of the sensing system. In addition, it should be mentioned that linear response of the output power of MI on the vibration amplitude will be ensured if vibration induced phase change locates in the linear region of a monotonic interval of the cosine transmission spectrum of MI, as indicated by Eq. (1), then it is able to measure the vibration amplitude quantitatively by monitoring the output power of MI. Finally it should be pointed out that it is possible to achieve multiple-point detection by using the MCF. In the case of long sensing range, distributed fiber sensing technique such as phase-sensitive optical time-domain reflectometer (ϕ -OTDR) can be implemented in one core of the MCF, so that ϕ -

OTDR can be used to locate different vibration points along the entire fiber, meanwhile the vibration frequencies can be measured by the interferometer.

4. Conclusions

In conclusion, we have proposed and demonstrated a simple and efficient optical fiber vibration sensor based on in-fiber spatially integrated Michelson interferometer using weakly coupled MCF. Vibration sensing with high sensitivity, high SNR and large frequency response range up to 12 kHz has been achieved, which is much higher than the values that are measured by the sensors that are made of strongly coupled MCF [10,11]. The dependence of MI performance on the selection of core pairs has been experimentally compared, and it turns out that MIs constructed using any two cores are able to retrieve the correct vibration frequency in the case of small vibration amplitude. Thanks to the unique structure of multiple separate cores embedded in the MCF, the proposed in-fiber integrated MI configuration possesses the advantages of temperature-insensitivity. Moreover, it does not need any special processing of the sensing fiber (e.g., tapering, splicing, etc.), therefore it possesses the advantages of compact and high mechanical strength. These advantages make the proposed fiber sensor more applicable in field installation than other alternative proposals. So it is believed that it will find many applications in vibration measurement.

Funding

GRF project PolyU (152168/17E and PolyU 152658/16E) of research grant council, Hong Kong SAR and 1-ZVGB, 1-YW3G, 1-YW0S, and H-ZG6B of the Hong Kong Polytechnic University; National Natural Science Foundation of China under Grants 61331010, 61722108, and 61435006.

Acknowledgments

We would like to thank Dr. Weijun Tong at Yangtze optical fibre and cable joint stock limited company (YOFC, China) for providing the multicore fiber.

References

1. Y. Li, X. Wang, and X. Bao, "Sensitive acoustic vibration sensor using single-mode fiber tapers," *Appl. Opt.* **50**(13), 1873–1878 (2011).
2. B. Xu, Y. Li, M. Sun, Z. W. Zhang, X. Y. Dong, Z. X. Zhang, and S. Z. Jin, "Acoustic vibration sensor based on nonadiabatic tapered fibers," *Opt. Lett.* **37**(22), 4768–4770 (2012).
3. Y. Xu, P. Lu, Z. Qin, J. Harris, F. Baset, P. Lu, V. R. Bhardwaj, and X. Bao, "Vibration sensing using a tapered bend-insensitive fiber based Mach-Zehnder interferometer," *Opt. Express* **21**(3), 3031–3042 (2013).
4. S. Dass and R. Jha, "Tapered fiber attached nitrile diaphragm-based acoustic sensor," *J. Lightwave Technol.* **35**(24), 5411–5417 (2017).
5. Y. Huang, T. Guo, C. Lu, and H. Y. Tam, "VCSEL-based tilted fiber grating vibration sensing system," *IEEE Photonics Technol. Lett.* **22**(16), 1235–1237 (2010).
6. Y. Weng, X. Qiao, T. Guo, M. Hu, Z. Feng, R. Wang, and J. Zhang, "A robust and compact fiber Bragg grating vibration sensor for seismic measurement," *IEEE Sens. J.* **12**(4), 800–804 (2011).
7. A. Wada, S. Tanaka, and N. Takahashi, "Optical fiber vibration sensor using FBG Fabry–Perot interferometer with wavelength scanning and Fourier analysis," *IEEE Sens. J.* **12**(1), 225–229 (2012).
8. B. Luo, W. Yang, X. Hu, H. Lu, S. Shi, M. Zhao, Y. Lu, L. Xie, Z. Sun, and L. Zhang, "Study on vibration sensing performance of an equal strength cantilever beam based on an excessively tilted fiber grating," *Appl. Opt.* **57**(9), 2128–2134 (2018).
9. Y. Ran, L. Xia, Y. Han, W. Li, J. Rohollahnejad, Y. Wen, and D. Liu, "Vibration fiber sensors based on SM-NC-SM fiber structure," *IEEE Photonics J.* **7**(2), 1–7 (2015).
10. J. Villatoro, E. Antonio-Lopez, J. Zubia, A. Schülzgen, and R. Amezcua-Correa, "Interferometer based on strongly coupled multi-core optical fiber for accurate vibration sensing," *Opt. Express* **25**(21), 25734–25740 (2017).
11. J. Villatoro, E. Antonio-Lopez, A. Schülzgen, and R. Amezcua-Correa, "Miniature multicore optical fiber vibration sensor," *Opt. Lett.* **42**(10), 2022–2025 (2017).
12. Y. Zhao, F. Xia, M. Chen, and R. Lv, "Optical fiber low-frequency vibration sensor based on butterfly-shape Mach-Zehnder interferometer," *Sens. Actuators A Phys.* **273**, 107–112 (2018).

13. Z. Zhao, Y. Dang, M. Tang, L. Duan, M. Wang, H. Wu, S. Fu, W. Tong, P. P. Shum, and D. Liu, "Spatial-division multiplexed hybrid Raman and Brillouin optical time-domain reflectometry based on multi-core fiber," *Opt. Express* **24**(22), 25111–25118 (2016).
14. W. C. Wong, C. C. Chan, L. H. Chen, Z. Q. Tou, and K. C. Leong, "Highly sensitive miniature photonic crystal fiber refractive index sensor based on mode field excitation," *Opt. Lett.* **36**(9), 1731–1733 (2011).
15. Z. Zhao, M. A. Soto, M. Tang, and L. Thévenaz, "Distributed shape sensing using Brillouin scattering in multi-core fibers," *Opt. Express* **24**(22), 25211–25223 (2016).
16. L. Yuan, "Recent progress of in-fiber integrated interferometers," *Photonic Sens.* **1**(1), 1–5 (2011).
17. B. Li, Z. Feng, M. Tang, Z. Xu, S. Fu, Q. Wu, L. Deng, W. Tong, S. Liu, and P. P. Shum, "Experimental demonstration of large capacity WSDM optical access network with multicore fibers and advanced modulation formats," *Opt. Express* **23**(9), 10997–11006 (2015).
18. M. Tang, Z. Zhao, L. Gan, H. Wu, R. Wang, B. Li, S. Fu, S. Liu, D. Liu, H. Wei, and W. Tong, "Spatial-division multiplexed optical sensing using MCF and FMF," in *Advanced Photonics*, paper SoM2G.3 (2016).